IEEE Access
Multidisciplinary | Rapid Review | Open Access Journal

Received February 10, 2019, accepted March 8, 2019, date of publication March 19, 2019, date of current version April 2, 2019.

Digital Object Identifier 10.1109/ACCESS.2019.2904697

Circularly Polarized Wideband-to-Narrowband Switchable Antenna

MOHAMMED E. YASSIN[1, 2], HESHAM A. MOHAMED[3], ESMAT A. F. ABDALLAH[3], AND HADIA S. EL-HENNAWY[2]

[1] Akhbar El Youm Academy, 6th of October City 12581, Egypt
[2]Faculty of Engineering, Ain Shams University, Cairo 11566, Egypt
[3]Electronics Research Institute, Giza 12622, Egypt

Corresponding author: Mohammed E. Yassin (el_be7ery@yahoo.com)

ABSTRACT This paper presents a circularly polarized printed wideband-to-narrowband switchable monopole antenna for UWB/WiMAX applications. The proposed switching antenna consists of circularly polarized monopole antenna for the UWB mode with two bandpass filters integrated into the feeding network for the two 3.5/5.5 GHz center frequencies narrowband modes. The proposed antenna is utilized to operate at triple modes; 7.3 GHz, 3.5 GHz, and 5.5 GHz with wide impedance bandwidth (117.6%, 16.7%, and 7.3%), wide axial ratio bandwidth (89.2%, 16.7%, and 7.3 %), and the gain reaches (6.91 dBi, 5.5 dBi, and 4.2 dBi).

INDEX TERMS UWB, monopole antenna, circular polarization, wideband-to-narrowband, reconfigurable, WiMAX.

I. INTRODUCTION

Recently, the rapid progress of the wireless technology increases the demand on devices able to operate at different standards. Moreover, the operation of cognitive radios and self-adaptive systems need to dynamically monitor the frequency spectrum in search of the unused licensed channels and then altering its radiation characteristics for transmission and reception within these spectrum holes as a second user for better exploit the existing spectrum [1], therefore the design of reconfigurable antennas has received much attention compared with conventional antennas, because it can provide diversity features in operating frequency [2], [3], polarization [4], [5], and/or radiation pattern [6], [7] to save size and cost for the multi-standard devices and cognitive radios.

The wideband-to-narrowband reconfigurable circularly polarized antennas are considered as the most suitable solution for the cognitive radio systems because it is able to switch between the ultra-wideband mode for sensing and multiple narrowband modes for communicating and the circular polarization allows signal reception irrespective of the orientation of transmit and receive antenna. The previous researchers carried out several methods to design the wideband-to-narrowband antennas [8]–[11]. An elliptical-shaped monopole antenna with two open loop bandpass filter and a three-pole hairpin band-pass filter in the feeding line is presented in [12]. The elliptical monopole able to produce the ultra-wideband mode, while the open loop and three-pole hairpin filters are responsible for 2.4/5.8 GHz WLAN narrowband modes, respectively. The antenna is able to switch between the modes by using five PIN diodes located in the feeding network. In [13], an annular ring monopole with a pair of stubs in the feeding line over a partial ground with a rectangular slit is presented. The proposed design is able to configure between the wideband mode and the narrowband mode by switching two PIN diodes integrated on the two stubs. An ellipse-shaped frequency reconfigurable antenna fed by a coplanar waveguide feeding line is introduced in [14]. The antenna is able to configure from the wideband mode to narrowband mode by switching two PIN diodes positioned at a pair of slot resonators etched in the ground. These previous antennas don't meet the portable/hand held devices because of its linear polarization, while in [15], a circularly polarized coplanar waveguide Archimedean spiral antenna is introduced. The proposed antenna consists of a two-arm spiral fed by a coplanar waveguide with a pair of meandered slot lines implemented in both sides and it is able to reconfigure from wideband mode to narrowband mode by switching a PIN diode integrated within the spiral element. The antenna is circularly polarized when operating at ultrawideband mode and linearly polarized when operating at the narrowband mode. While in [16], a two port circularly polarized reconfigurable antenna is presented. The antenna consists of two

The associate editor coordinating the review of this manuscript and approving it for publication was Roberto Gomez-Garcia.

triangle monopole antennas connected with a narrow link to produce a circular polarization operation. The antenna can support both RHCP and LHCP operations in single wideband (1.6-2.56 GHz) and dual-band (1.25/2.43 GHz) modes by using four PIN diodes locating in the links and the feed lines of the two ports. Also, in [17], a frequency reconfigurable circularly polarized slot antenna is proposed. The antenna consists of annular slot fed by a shorted microstrip line through coupling. The antenna can be reconfigured between two operating frequencies of 1.88 GHz with bandwidth ratio of 2.7% and 2.88 GHz with bandwidth ratio of 3.3% by controlling the dc voltage of the varactor placed on the slot. The antennas in [16] and [17] are circularly polarized at all modes, but the wideband mode bandwidth isn't sufficient for the sensing process of the cognitive radio devices.

In this paper, a wideband-to-narrowband switchable antenna with wideband circular polarization for all modes is designed. The antenna consists of an ultra-wideband circularly polarized monopole patch with two bandpass filters integrated in the feeding network used to switch between wideband mode to two narrowband modes. The proposed antenna is designed to achieve a good bandwidth, axial ratio and radiation characteristics to cover ultra-wideband applications at the ultrawideband mode and WiMAX at the two narrowband modes. The antenna is designed and studied using Computer Simulation Technology (CST) software. The paper is organized as follows: The detailed design and structure are described in section 2. Section 3 presents the simulation and measurement results. Finally, the conclusions are introduced in section 4.

II. DESIGN AND STRUCTURE

The geometry of the proposed wideband-to-narrowband antenna is shown in Fig. 1. The antenna is printed over the two-sides of Rogers 4003C substrate with a relative permittivity of 3.38, 0.41 mm thickness, and a loss tangent of 0.0027 with a total area of 45 × 50 mm^2. The proposed antenna consists of three parts: The circularly polarized monopole antenna for the ultra-wideband mode (part A), three-line coupled resonator bandpass filter centered at 3.5 GHz for the first narrowband mode (part B) and two open-loop resonators bandpass filter centered at 5.5 GHz for the second narrowband mode (part C). The two filters are merged with the tapered feeding line of the monopole antenna. The antenna is capable of configuring between the ultra-wideband mode and the two narrow band modes by selecting different RF paths. The switching between the modes is controlled by using Mini-Circuits RF switch matrix RC-8SPDT-A18 (which is the replacement of PIN diodes or RF-MEMS). When the RF signal is fed directly to the monopole antenna the ultra-wideband mode is achieved, while the first and second narrowband modes can be achieved by selecting the RF signal to pass to the monopole through the 3.5 GHz three-line coupled resonator band-pass filter and 5.5 GHz two open-loop resonators band-pass filter, respectively.

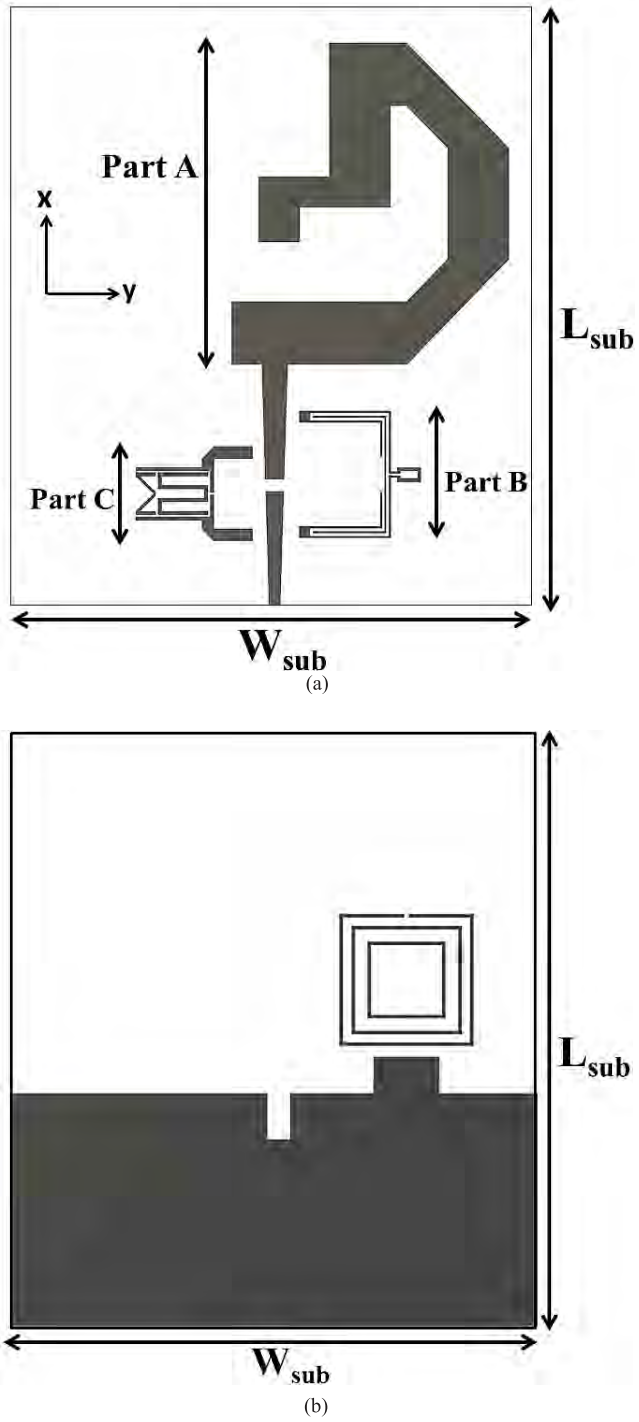

FIGURE 1. The design of wideband-to-narrowband antenna (a) Front view, and (b) back view.

A. UWB CIRCULARLY POLARIZED ANTENNA

The main radiator of the proposed antenna is an ultra-wideband circularly polarized monopole antenna. The circular polarization allows wave reception with minimum polarization loss regardless of the transmitter and the receiver antennas orientations and reduces the multipath reflections effect which gives a freedom of mobility to the transmitting and receiving devices. For these reasons the circular

polarization antennas are becoming a key technology for many wireless communication systems including worldwide interoperability for microwave access (WiMAX) and cognitive radio (CR). The main challenge in the wideband applications is the trade-off between the impedance bandwidth (IBW) and the axial ratio bandwidth (AR-BW). The basic microstrip antenna shapes produce linear polarization [18]–[20], so that perturbation segments with optimized shape and dimensions should be added to the antenna to achieve circular polarization using a single feed. The previous researchers developed several methods to design a CP antenna which is able to cover the ultra- wideband frequency range [21].

In [22], a L-shaped strip and inverted L-shaped strip combined at the radiating edge of the rectangular monopole which was designed to produce a CP wideband characteristic. The proposed antenna achieves IBW of 133.41% (1.38-6.91 GHz) and AR-BW of 129.04% (1.38-6.4 GHz). A semi-circular patch antenna with a circular slot on ground is introduced in [23]. The antenna achieves IBW of 116.6% (2.37-9 GHz) and AR-BW of 58.7% (3.22-5.9 GHz). A C-shaped monopole with a partial ground modified with two triangle stubs is proposed in [24]. The antenna has 106.3% (2.25-7.35 GHz) IBW and 104.7% (2.05-6.55 GHz) AR-BW.

Fig. 2 shows the proposed ultra-wideband circularly polarized monopole antenna. The antenna consists of eight microstrip segments to form a 24 × 27 mm^2 quasi C-shaped monopole fed with a linear tapered line used to match the radiator with the 50-ohm port and on the other side of the substrate a partial ground modified by a rectangular slit and a rectangular stub with one split ring resonator and two square ring resonators are printed. The dimensions of the antenna are listed in table 1.

In order to explain the procedure of the antenna design, four antennas (Ant. 1-4) are illustrated in Fig. 3, while Fig. 4 shows the reflection coefficient and axial ratio simulation results of the four antennas (Ant.1-4). As shown in Fig.4(a), the quasi C-shaped conventional monopole (Ant.1) produces its fundamental resonance at 3.63 GHz and the length of the monopole is about quarter wavelength at its resonance frequency. By using the rectangular slit (Ant.2) a new resonance has been added at 6.2 GHz which expands the IBW from 5.7 GHz to 10.9 GHz, while adding the rectangular stub and three-square resonators with an edge of quarter wavelength at its resonance frequency in step 3 can excite extra resonance at 6.5 GHz which can improve the impedance matching at higher band. For the simulated axial ratio shown in Fig.4(b), the quasi C-shaped radiator in step 1 can provide the perturbation of current distributions in X and Y directions due to its curved structure. Thus, CP operation can be realized by splitting the fundamental resonant mode into two near-degenerate modes along the orthogonal arms of the quasi C-shaped monopole. Moreover, the main function of the rectangular slit added on the ground in step 2 is to change the surface current distributions balanced on the unmodified ground in step1, so that a single CP mode is excited

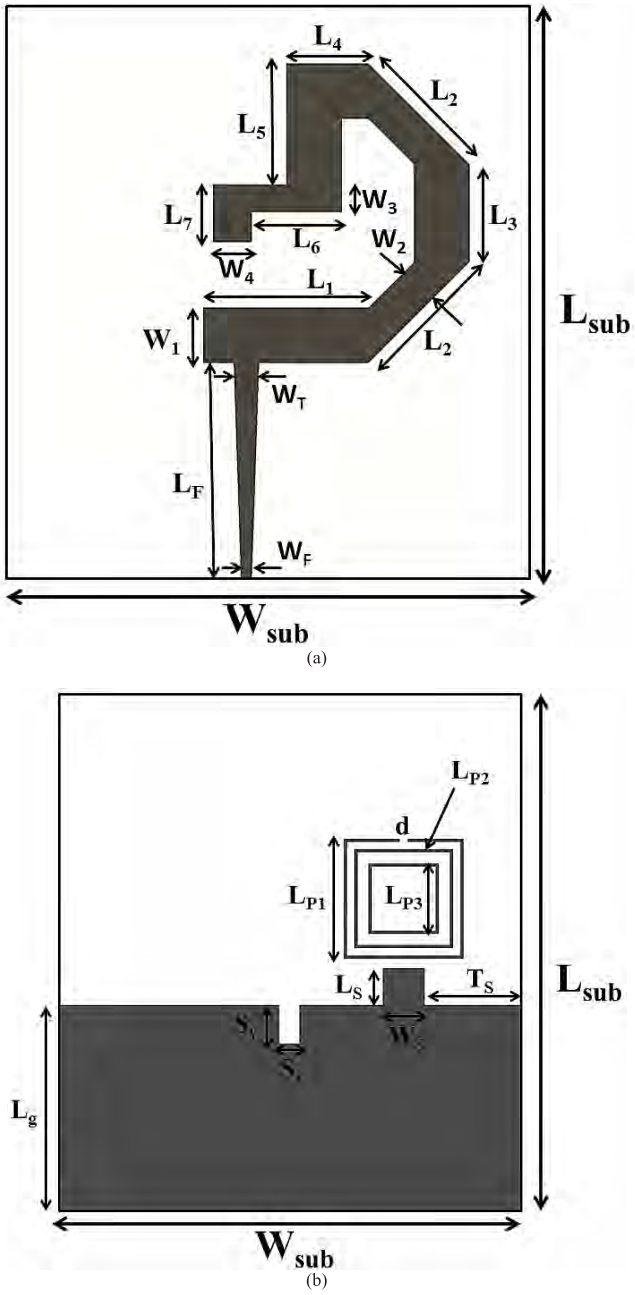

FIGURE 2. The design of quasi C-shaped monopole antenna (a) Front view, and (b) back view.

at 5.5 GHz. The resonators considered offset-coupled with the C-shaped monopole, while the rectangular stub can be used to couple with the open-loop and the C-shaped monopole, so that by adjusting the dimensions and positions of the square resonators and the rectangular stub embedded on the ground plane in step 3 (Ant.3), a CP mode can be excited at 6.5 GHz by properly proximity coupling of the C-shaped monopole and the resonators which improves the AR at the higher band. The combination of step 2 and step 3 makes the proposed design (step 4) which achieves IBW of 109.22% (3.2-10.9 GHz) and AR-BW of 89.59% (3.05-8 GHz).

TABLE 1. Monopole antenna dimensional parameters.

Parameter	Value(mm)	Parameter	Value(mm)
L_{sub}	50	W_2	3.7
W_{sub}	45	W_3	2.5
L_f	20	W_4	3.5
L_1	14.9	W_S	4
L_2	12.9	L_s	3.5
L_3	8.8	L_g	19.9
L_4	7.4	S_x	1.9
L_5	10.9	S_y	3.7
L_6	6.6	L_{p1}	11.4
L_7	5.2	L_{p2}	9.4
W_F	0.95	L_{p3}	6.7
W_T	2.3	d	0.8
W_1	5	T_S	9.6

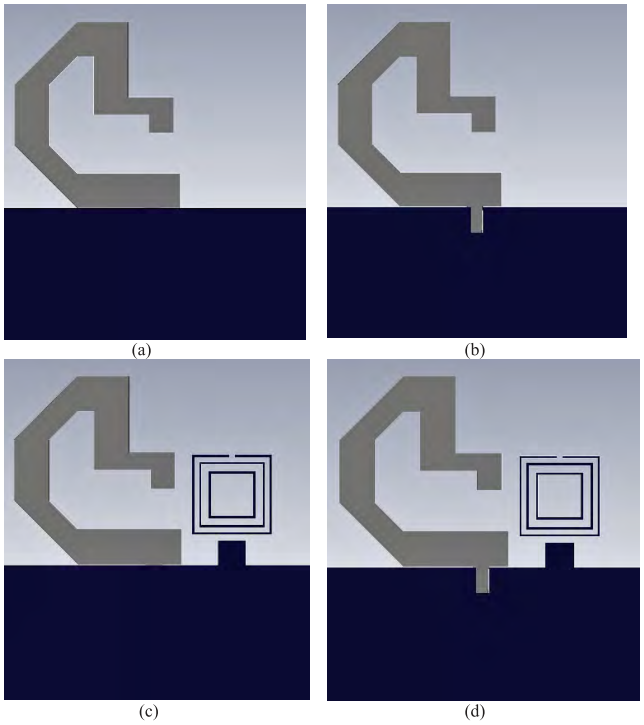

FIGURE 3. The design procedure of the proposed antenna (a) step 1, (b) step 2, (c) step 3, and (d) step 4.

For further explanation of the operation of the CP mechanism, Fig. 5 shows the simulated surface current distribution at 5.5 GHz for the phases of 0°, 90°, 180° and 270°. In this figure, the red arrow represents the direction of the predominant surface current which rotates counterclockwise. Hence, right-hand CP (RHCP) waves in the broadside direction (+Z axis) can be excited.

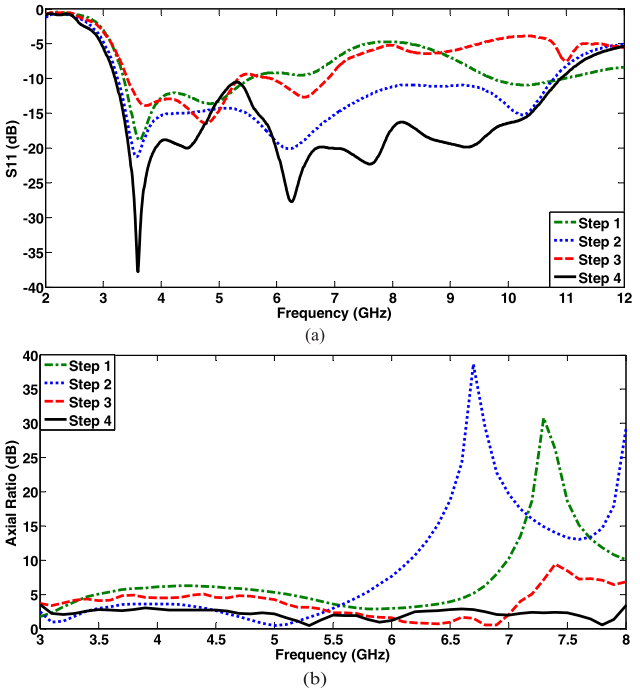

FIGURE 4. The simulated results for step 1-4 (a) return loss, and (b) axial ratio.

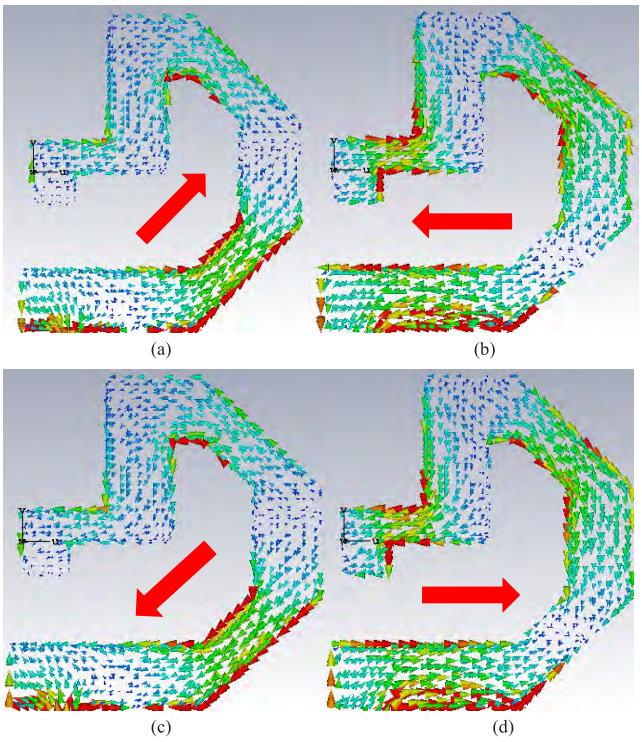

FIGURE 5. Simulated surface current distributions of the proposed antenna at 5.5 GHz at four different phases (a) 0°, (b) 90°, (c) 180°, (d) 270°.

B. MODIFIED THREE-LINE COUPLED RESONATOR BPF

A modified compact microstrip three-line coupled resonator (TLCR) bandpass filter is inserted in the feeding line of the UWB monopole antenna by using switching matrix

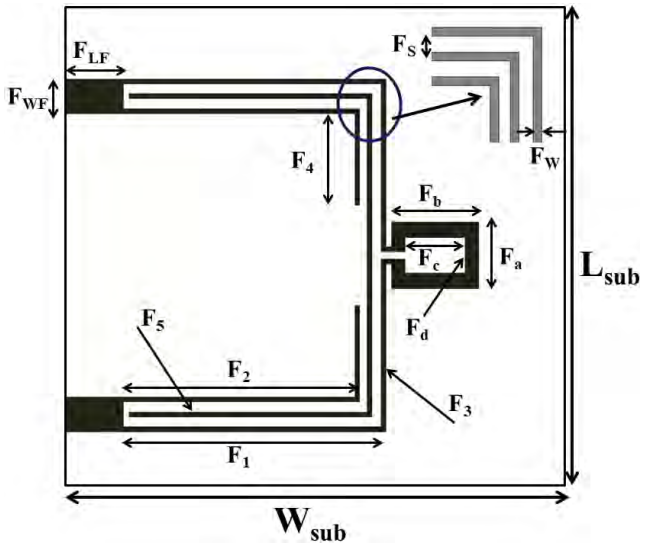

FIGURE 6. The design of TLCR bandpass filter.

TABLE 2. The modified TLCR filter dimensional parameters.

Parameter	Value (mm)	Parameter	Value (mm)
L_{sub}	16	F_3	9.2
W_{sub}	15	F_4	2.6
F_{LF}	2	F_5	6.95
F_{WF}	1	F_a	1.9
F_W	0.15	F_b	2.5
F_S	0.275	F_c	1.7
F_1	7.5	F_d	1
F_2	6.6		

equipment to generate the first narrowband mode centered at 3.5 GHz. The TLCR bandpass filter has the advantages of simple structure, compact size and wide passband. In [25], a shorting to ground using via is used with two of the outer coupled lines to produce one transmission zero at each edge of the passband. Also, a pair of open-ended stubs are attached at the center to increase the filter degree. To increase the selectivity in [26], a T-shaped open stub is added to a U-shaped TLCR which added two resonance modes in the passband and two transmission zeros at the passband boundaries. A dual-wideband TLCR bandpass filter achieved by using a resonator with a meandering stub is presented in [27]. In this paper the proposed filter is shown in Fig. 6, it is constructed of U-shaped two sections of three coupled microstrip lines. The length of the coupled lines equals to a quarter of the wavelength at the center frequency. A rectangular loop resonator is added to the filter to generate additional resonance to the passband in order to achieve wider passband bandwidth. The filter has total area of 16×15 mm^2 and the dimensions are listed in table 2, all dimensions in mm.

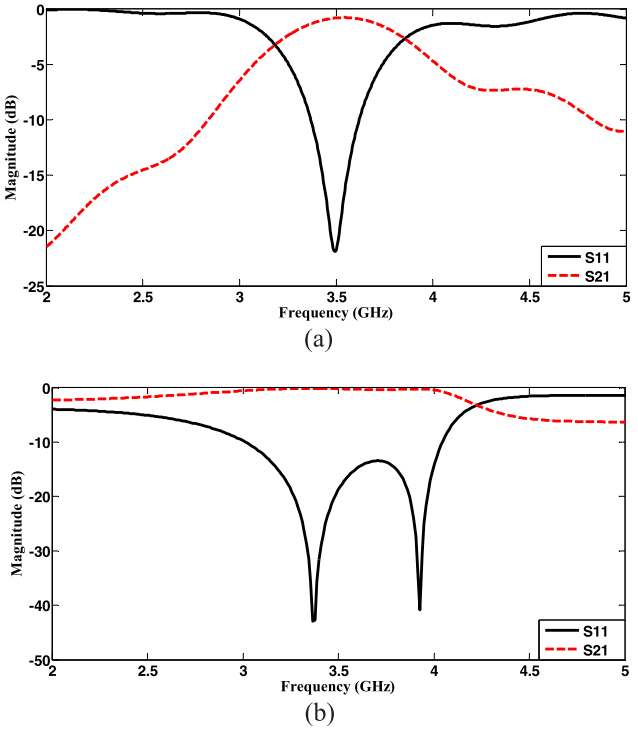

FIGURE 7. The simulation results of the TLCR bandpass filters (a) Traditional U-shaped TLCR, and (b) Modified TLCR.

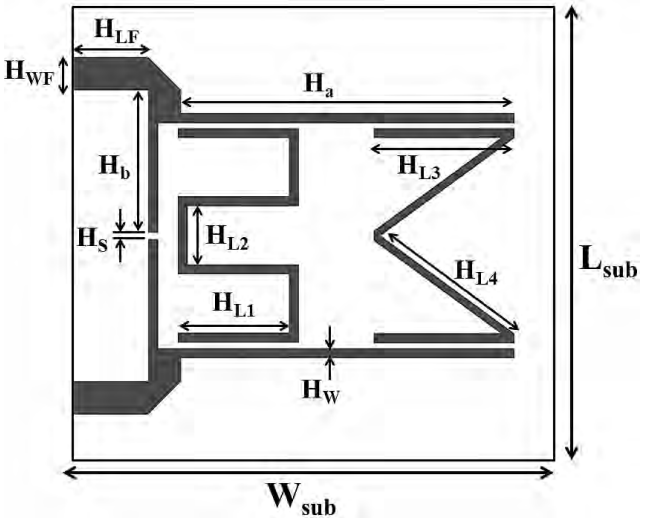

FIGURE 8. The design of the two resonators wideband BPF.

Fig. 7 shows the results of the traditional U-shaped TLCR and the proposed modified TLCR filter simulated using Computer Simulation Technology (CST) software. The results show that the filter provides −10 dB passband bandwidth of 1.05 GHz (3-4.05 GHz), while the insertion loss in the passband is less than 0.56 dB. The combination between the traditional TLCR filter with the additional resonance of the square loop resonator achieves ultrawide and deep passband bandwidth with a good sharpness factor by adding a second resonance in the passband.

TABLE 3. Dimensions of the proposed filter.

Variable	Value (mm)	Variable	Value (mm)
L_{sub}	12.8	H_{L1}	3.4
W_{sub}	16	H_{L2}	1.76
H_{LF}	2.5	H_{L3}	4.3
H_{WF}	1	H_{L4}	5.3
H_W	0.3	H_a	10.2
H_S	0.2	H_b	4.3

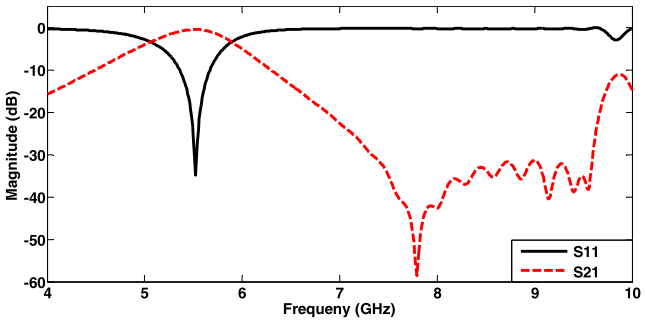

FIGURE 9. The simulation results of the two resonators wideband bandpass filter.

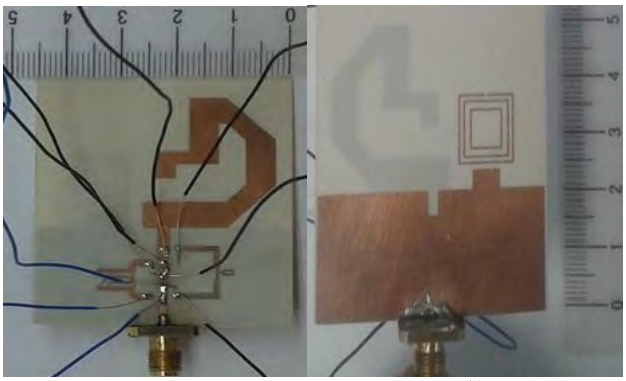

FIGURE 10. Photograph of fabricated antenna. (a) Front view, and (b) back view.

C. WIDEBAND BPF USING TWO RESONATORS

The third part of the wideband-to-narrowband antenna system is a wideband bandpass filter using two open loop resonators for a passband centered at 5.5 GHz to select the second narrowband mode. In [28] a U-shaped and a folded U-shaped open loop resonator are used to produce two transmission zeros at the passband's upper frequency area. To produce dual-band behavior with high isolation and a wide stopband in [29], two identical stub-loaded resonators at left and right sides and a different stub-loaded resonator at the middle are used. A compact wideband bandpass filter with an improved upper stopband is presented in [30]. The improvement of the upper stopband is realized by adding three transmission zeros using different open/short stubs. In this paper the proposed filter is shown in Fig. 8, it is constructed of U-shaped filter

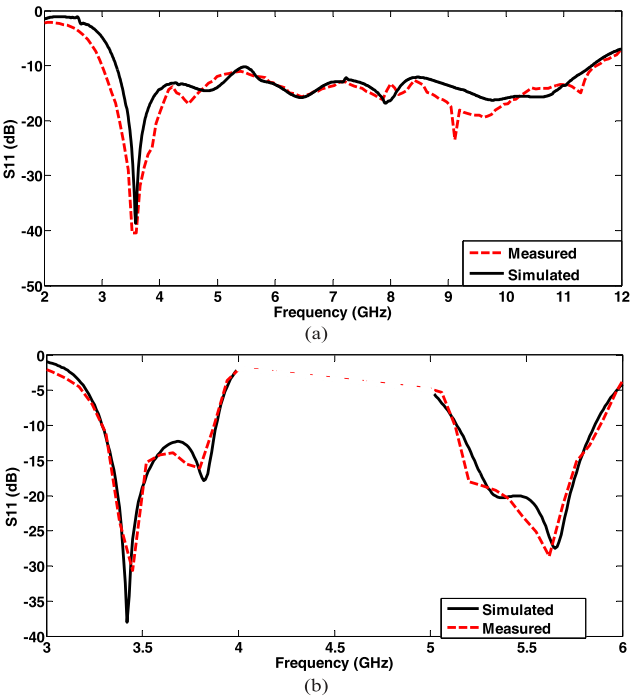

FIGURE 11. The simulated and measured reflection coefficient of the different modes of the antenna (a) UWB mode, and (b) NB modes.

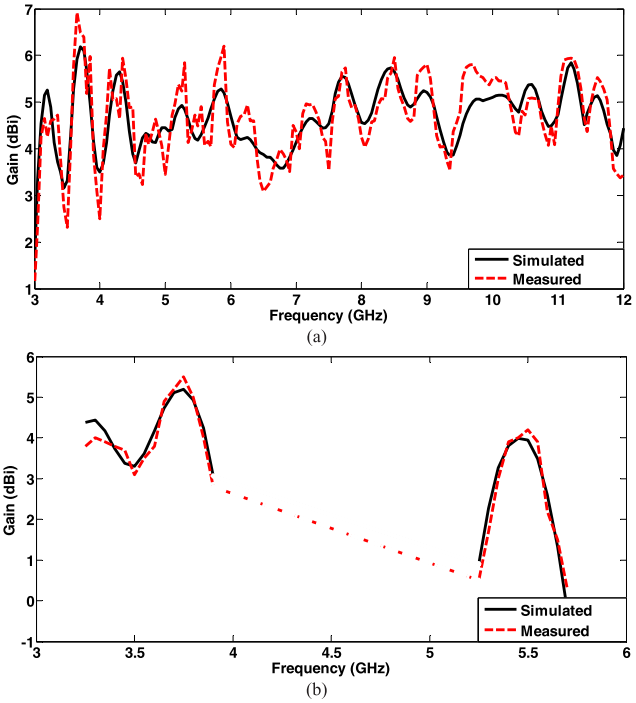

FIGURE 12. The simulated and measured realized gain of the different modes of the antenna (a) UWB mode, and (b) NB modes.

with two open loop resonators. The wideband behavior is mainly dependent on the M-shaped open loop resonator, while the other resonator is used to improve the performance, especially adding transmission zeros in the upper stopband. The filter has total area of 12.8×16 mm^2 and the dimensions are listed in table 3.

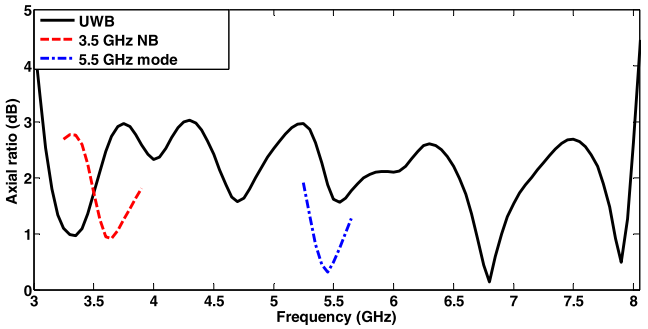

FIGURE 13. The simulated axial ratio of the different modes of the antenna.

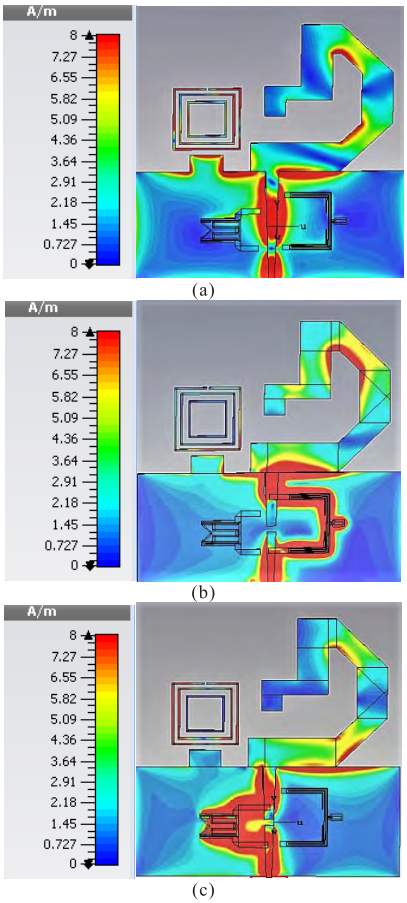

FIGURE 14. Simulated current distribution for (a) the UWB mode at 7.3 GHz, (b)the first NB mode at 3.5 GHz, and (c) the second NB mode at 5.5 GHz.

Fig. 9, shows the results of the proposed filter simulated using CST. The results show that the filter provides a passband centered at 5.47 GHz with 16.4% bandwidth and the return loss is under −10 dB over 34.4% of the passband, while the insertion loss has more than 30 dB of spurious suppression in the upper stopband from 7.3 GHz to 9.6 GHz.

III. SIMULATION AND MEASUREMENT RESULTS

Based on the above, the antenna has been fabricated using the photolithographic technique. Fig. 10 shows a photograph of the fabricated antenna. The input reflection coefficient has been measured using a ROHDE&SCHWARZ ZVA 67 vector network analyzer, while the radiation pattern and gain have been measured using anechoic chamber NSI 700S-30.

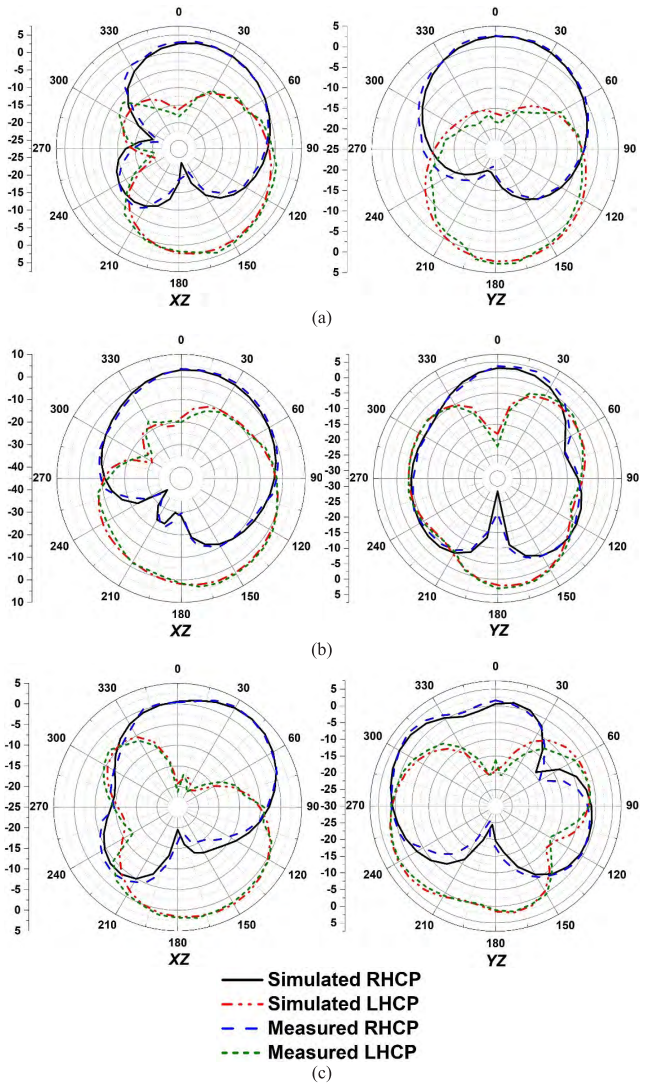

FIGURE 15. The measured and simulated Normalized co-polar and cross-polar patterns of the proposed antenna in XZ and YZ planes for (a) the first NB mode at 3.5 GHz, (b) the second NB mode 5.5 GHz, and (c) the UWB mode at 7.3 GHz.

The simulation and measurement results are illustrated in Fig. 11-13. The UWB mode of the proposed antenna achieves an impedance bandwidth of 8.57 GHz (3-11.57 GHz), a 3-dB axial ratio bandwidth of 4.94 GHz (3.07-8.01 GHz) with 6.91 dBi peak gain and 4.69 dBi average gain, while the first narrowband mode has an impedance and axial ratio bandwidths of 600 MHz (3.29-3.89 GHz) with 5.5 dBi peak gain and 4.18 dBi average gain, which is sufficient to cover WiMAX at 3.5 GHz. Moreover, the second narrowband mode has an impedance and axial ratio bandwidths of 400 MHz (5.25-5.65 GHz) with 4.2 dBi peak gain and 2.85 dBi average gain, which covers the WiMAX at 5.5 GHz.

For further explanation of the operation of the wideband-to-narrowband antenna, the excited surface current

TABLE 4. Comparison of proposed wideband-to-narrowband switchable antenna with those existing in the literature.

Ref.	Dielectric constant	Size (mm x mm)	Sensing band -10 dB IBW GHz	Sensing band 3 dB AR-BW GHz	Communications band -10 dB IBW GHz	Communications band 3 dB AR-BW GHz
[9]	4.9	144 x 140	1-3.2	N	1.1-1.3/2.1-2.25/2.7-3.2	N
[10]	3.5	75.7 x 58.35	2.1-12	N	4.4-5.4/6.4-7.6	N
[11]	4.3	88 x 88	2-6	N	2.3-2.45/3.4-3.6/4.95-5.7	N
[12]	4.4	45 x 40	2.2-11	N	2.4-2.6 / 5-6.2	N
[13]	4.4	40.15 x 40.15	3.1-10.6	N	5.13-6.47	N
[14]	4.7	49 x 35	3.5-5.97	N	5.6-5.9	N
[15]	4.6	60 x 69	2-8	2-3.2	5.1-5.9	N
[16]	4.4	50 x 50	1.6-2.56	1.62-2.55	1.25-1.3/2.1-2.6	1.25-1.3/2.1-2.6
This Work	3.38	45 x 50	3-11.57	3.1-8	3.29-3.89 / 5.25-5.65	3.29-3.89 / 5.25-5.65

distributions of the different modes are simulated at the resonance frequencies 7.3 GHz, 3.5 GHz and 5.5 GHz, respectively. At the UWB mode, the RF signal is fed directly to the monopole antenna to generate the UWB behavior as shown in Fig. 14(a), while Fig. 14(b) shows the current distribution at 3.5 GHz, the first narrow band is generated by feeding the RF signal to the monopole antenna through the TLCR bandpass filter. The second narrowband mode is generated by feeding the RF signal to the monopole antenna through the two resonators bandpass filter as shown in Fig. 14(c).

Fig. 15 shows the measured and simulated antenna normalized co-polar (RHCP) and cross-polar (LHCP) radiation patterns in XZ and YZ planes at the center frequencies of the three modes 3.5 GHz, 5.5 GHz and 7.3 GHz. The proposed antenna is a bidirectional radiator with RHCP wave in +Z direction and LHCP wave in –Z direction for the three modes.

IV. CONCLUSION

A wideband-to-narrowband antenna was proposed. The antenna consists of a circularly polarized ultrawideband monopole as a main radiator and two bandpass filters integrated in the feeding network. The switching between the wideband mode and the two narrowband modes is achieved by selecting the RF signal directly to the monopole antenna or through one of the two bandpass filters using mini-circuit switching matrix equipment. The proposed antenna is utilized to operate at triple modes; 7.3 GHz, 3.5 GHz and 5.5 GHz with wide impedance bandwidth (117.6%, 16.7%, and 7.3%), wide axial ratio bandwidth (89.2%, 16.7%, and 7.3 %) and high gain (6.91 dBi, 5.5 dBi, 4.2 dBi).

REFERENCES

[1] K.-C. Chen and R. Prasad, *Cognitive Radio Networks*. Hoboken, NJ, USA: Wiley, 2009.

[2] Y. M. Cai, K. Li, Y. Yin, S. Gao, W. Hu, and L. Zhao, "A low-profile frequency reconfigurable grid-slotted patch antenna," *IEEE Access*, vol. 6, pp. 36305–36312, 2018.

[3] N. Nguyen-Trong, A. Piotrowski, and C. Fumeaux, "A frequency-reconfigurable dual-band low-profile monopolar antenna," *IEEE Trans. Antennas Propag.*, vol. 65, no. 7, pp. 3336–3343, Jul. 2017.

[4] S. W. Lee and Y. J. Sung, "Simple polarization-reconfigurable antenna with T-shaped feed," *IEEE Antennas Wireless Propag. Lett.*, vol. 15, pp. 114–117, 2016.

[5] K. X. Wang and H. Wong, "A reconfigurable CP/LP antenna with cross-probe feed," *IEEE Antennas Wireless Propag. Lett.*, vol. 16, pp. 669–672, 2017.

[6] H.-W. Deng, T. Xu, and F. Liu, "Broadband pattern-reconfigurable filtering microstrip antenna with Quasi–Yagi structure," *IEEE Antennas Wireless Propag. Lett.*, vol. 17, no. 7, pp. 1127–1131, Jul. 2018.

[7] P. K. Li, Z. H. Shao, Q. Wang, and Y. J. Cheng, "Frequency- and pattern-reconfigurable antenna for multistandard wireless applications," *IEEE Antennas Wireless Propag. Lett.*, vol. 14, pp. 333–336, 2014.

[8] P. Y. Qin, F. Wei, and Y. J. Guo, "A wideband-to-narrowband tunable antenna using a reconfigurable filter," *IEEE Trans. Antennas Propag.*, vol. 63, no. 5, pp. 2282–2285, May 2015.

[9] M. R. Hamid, P. Gardner, P. S. Hall, and F. Ghanem, "Switched-band Vivaldi antenna," *IEEE Trans. Antennas Propag.*, vol. 59, no. 5, pp. 1472–1480, May 2011.

[10] P. Sasmita and S. Sudhakar, "A two port UWB-dual narrowband antenna for cognitive radios," *Microw. Opt. Technol. Lett.*, vol. 58, no. 8, pp. 1973–1978, 2016.

[11] I. H. Idris, M. R. Hamid, K. Kamardin, and M. K. A. Rahim, "A multi to wideband frequency reconfigurable antenna," *Int. J. RF Microw. Comput. Aided Eng.*, vol. 28, no. 4, 2017, Art. no. e21216.

[12] J. Deng, S. Hou, L. Zhao, and L. Guo, "Wideband-to-narrowband tunable monopole antenna with integrated bandpass filters for UWB/WLAN applications," *IEEE Antennas Wireless Propag. Lett.*, vol. 16, pp. 2734–2737, 2017.

[13] E. J. B. Rodrigues, H. W. Lins, and A. G. D'Assunção, "Fast and accurate synthesis of electronically reconfigurable annular ring monopole antennas using particle swarm optimisation and artificial bee colony algorithms," *IET, Antennas Propag.*, vol. 10, no. 4, pp. 362–369, Mar. 2016.
[14] M. C. Lim, S. K. A. Rahim, M. R. Hamid, A. A. Eteng, and M. F. Jamlos, "Frequency reconfigurable antenna for WLAN application," *Microw. Opt. Technol. Lett.*, vol. 59, no. 1, pp. 171–176, 2017.
[15] F. D. Dahalan *et al.*, "Frequency-reconfigurable archimedean spiral antenna," *IEEE Antennas Wireless Propag. Lett.*, vol. 12, pp. 1504–1507, 2013.
[16] I. H. Idris, M. R. Hamid, K. Kamardin, and M. K. A. Rahim, "A multi to wideband frequency reconfigurable antenna," *Int. J. RF Microw. Comput. Aided Eng.*, vol. 28, no. 4, 2018, Art. no. e21216.
[17] C.-C. Wang, M.-Y. Chen, and J.-S. Row, "Circularly polarized annular slot antenna with switchable frequency," *Microw. Opt. Technol. Lett.*, vol. 55, pp. 1115–1118, May 2013.
[18] P. Wang, G.-J. Wen, Y.-J. Huang, and Y.-H. Sun, "Compact CPW-fed planar monopole antenna with distinct triple bands for WiFi/WiMAX applications," *Electron. Lett.*, vol. 48, no. 7, pp. 357–359, Mar. 2012.
[19] C. H. See, R. A. Abd-Alhameed, Z. Z. Abidin, N. J. McEwan, and P. S. Excell, "Wideband printed MIMO/diversity monopole antenna for WiFi/WiMAX applications," *IEEE Trans. Antennas Propag.*, vol. 60, no. 4, pp. 2028–2035, Apr. 2012.
[20] D. Li and J.-F. Mao, "Coplanar waveguide-fed Koch-like sided Sierpinski hexagonal carpet multifractal monopole antenna," *IET Microw., Antennas Propag.*, vol. 8, no. 5, pp. 358–366, Apr. 2014.
[21] H. Mextorf, R. Martens, F. Daschner, and R. Knöchel, "Dual polarized UWB antenna for free-space characterization of dielectric objects," in *German Microw. Conf. Dig. Papers*, Berlin, Germany, Mar. 2010, pp. 162–165.
[22] D. S. Chandu and S. S. Karthikeyan, "Broadband circularly polarized printed monopole antenna with protruded L-shaped and inverted L-shaped strips," *Microw. Opt. Technol. Lett.*, vol. 60, pp. 242–248, Jan. 2018.
[23] T. T. Le, V. H. The, and H. C. Park, "Simple and compact slot-patch antenna with broadband circularly polarized radiation," *Microw. Opt. Technol. Lett.*, vol. 58, no. 7, pp. 1634–1641, 2016.
[24] H. Tang, K. Wang, R. Wu, C. Yu, J. Zhang, and X. Wang, "A novel broadband circularly polarized monopole antenna based on C-shaped radiator," *IEEE Antennas Wireless Propag. Lett.*, vol. 16, pp. 964–967, 2017.
[25] H. N. Shaman, "New S-band bandpass filter (BPF) with wideband passband for wireless communication systems," *IEEE Microw. Wireless Compon. Lett.*, vol. 22, no. 5, pp. 242–244, May 2012.
[26] S. J. Borhani, M. A. Honarvar, and B. S. Virdee, "High selectivity UWB bandpass filter with a wide notched-band," *Microw. Opt. Technol. Lett.*, vol. 57, pp. 634–639, Mar. 2015.
[27] K.-W. Hsu, C.-H. Chien, and W.-H. Tu, "Compact dual-wideband bandpass filter using asymmetrical resonator," *Electron. Lett.*, vol. 49, no. 2, pp. 123–124, Jan. 2013.
[28] X.-B. Ma and H.-X. Zheng, "Compact wideband bandpass filter using two open loop resonators," *Microw. Opt. Technol. Lett.*, vol. 55, pp. 915–917, Apr. 2013.
[29] Y. Xie, F.-C. Chen, and Z. Li, "Design of dual-band bandpass filter with high isolation and wide stopband," *IEEE Access*, vol. 5, pp. 25602–25608, 2017.
[30] K. Deng and W. Feng, "Wideband bandpass filter with multiple transmission zeros and compact size," *Microw. Opt. Technol. Lett.*, vol. 58, pp. 2452–2456, Oct. 2016.

MOHAMMED E. YASSIN received the B.Sc. degree in electronics and communication engineering from Akbar El Youm Academy (AYA), 6 of October city, Giza, Egypt, in 2006, and the M.Sc. degree from Ain Shams University, in 2012. He is currently an Assistant Teacher with the Electronics and Communications Department, Akbar El Youm Academy. His research interests include microwave circuit designs and power amplifiers, and recently on microwave filters, UWB antennas, circularly polarized antennas, filtering antennas, and reconfigurable antennas.

HESHAM A. MOHAMED received the B.Sc. degree in electronics and communication engineering from the University of Menofia, in 2003, and the M.Sc. and Ph.D. degrees from Ain Shams University, in 2009 and 2014 respectively. He is currently a Researcher with the Electronics Research Institute (ERI), Giza, Egypt. He is also a Lecturer with the Electronic and Communication Engineering Department, Faculty of Engineering, Misr University for Science and Technology. His research interests include radar absorbing materials, energy harvesting and wireless power transfer, smart antennas, microstrip antennas, microwave filters, metamaterials, and MIMO antennas and its applications in wireless communications.

ESMAT A. F. ABDALLAH received the degree from the Faculty of Engineering and the M.Sc. and Ph.D. degrees from Cairo University, Giza, Egypt, in 1968, 1972, and 1975, respectively. She was nominated as an Assistant Professor, an Associate Professor, and a Professor, in 1975, 1980, and 1985, respectively. In 1989, she was appointed as a President of the Electronics Research Institute (ERI), Cairo, Egypt, a position she held for about ten years. She became the Head of the Microstrip Department, ERI, from 1999 to 2006. She is currently with the Microstrip Department, ERI. She has focused her research on microwave circuit designs, planar antenna systems, and nonreciprocal ferrite devices, and recently on EBG structures, UWB components and antenna and RFID systems. She acts as a single author and as a co-author on more than 160 research papers in highly cited international journals and in proceedings of international conferences in her field.

HADIA S. EL-HENNAWY received the B.Sc. and the M.Sc. degrees from Ain Shams University, Cairo, Egypt, in 1972 and 1976, respectively, and the Ph.D. degree from the Technische Universitat Braunschweig, Germany, in 1982. In 1982, she returned to Egypt and joined the Electronics and Communications Engineering Department, Ain Shams University, as an Assistant Professor. She was nominated as an Associate Professor, in 1987, and then a Professor, in 1992. In 2004, she was appointed as the Vice-Dean for graduate study and research. In 2005, she was appointed as the Dean of the Faculty of Engineering, Ain Shams University. She has been the Head of the Microwave Research Laboratory, Ain Shams University, since 1982. She has published more than 100 journal and conference papers and supervised more than 50 Ph.D. and M.Sc. students. She has focused her research on microwave circuit design, antennas, microwave communication, and recently wireless communication. She is a member of the Industrial Communication Committee in the National Telecommunication Regulatory Authority (NTRA), Educational Engineering Committee in the Ministry of Higher Education, and Space Technology Committee in the Academy of Scientific Research. She was the Editor-in-Chief of the Faculty of Engineering, Ain Shams University, Scientific Bulletin, from 2004 to 2005. She is deeply involved in the Egyptian branch activities.